Available online at www.sciencedirect.com
SCIENCE DIRECT®
Journal of Solid State Chemistry 178 (2005) 761–768
JOURNAL OF SOLID STATE CHEMISTRY
www.elsevier.com/locate/jssc

Rapid synthesis of ultrafine $K_2Ln_2Ti_3O_{10}$ (Ln = La, Nd, Sm, Gd, Dy) series and its photoactivity

LiLi Zhang[a,b], Weiguang Zhang[a,b], Junwu Zhu[a], LuDe Lu[a,*], Xujie Yang[a], Xin Wang[a]

[a]*Materials Chemistry Laboratory, Center of Nanoscience and Nanotechnology, Nanjing University of Science and Technology, Nanjing 210094, P.R. China*
[b]*Department of Chemistry, Huaiyin Teachers College, Huai'an 223001, P.R. China*

Received 18 September 2004; received in revised form 8 December 2004; accepted 10 December 2004

Abstract

Ultrafine-layered lanthanon titanates $K_2Ln_2Ti_3O_{10}$ (Ln = La, Nd, Sm, Gd, Dy) were fabricated at relatively low temperature by a stearic acid method (SAM). The obtained products were characterized by FT-IR, X-ray diffractometer, DTA–TG, scanning electron microscopy, transmission electron microscopy and BET experiments. The photocatalytic activity of the obtained products was studied and was compared with that of solid-state reaction (SSR) using photodecomposition of methyl orange as the model system. Results showed that by using SAM, the fabricating temperature was lowered (from 1100 to 800 °C) and the reacting time was shortened (from at least 11–2 h). Comparing with the product of traditional SSR, the particle size of $K_2Ln_2Ti_3O_{10}$ synthesized by SAM is smaller, BET surface area is higher (more than 16.97 m^2/g), and photoreactivity is better. It was very interesting to find the difference in d(002) of obtained $K_2Ln_2Ti_3O_{10}$ for Ln = La, Nd, Sm, Gd, Dy separately and the photoactivity of $K_2Ln_2Ti_3O_{10}$ is strongly dependent on lanthanide, increasing in the sequence of La < Sm < Nd < Gd < Dy. A possible reason was put forward.

Keywords: Layered lanthanon titanates; Stearic acid method; Photocatalytic sequence

1. Introduction

Peculiar properties differing from bulk materials may appear as the dimensions of materials are reduced to the submicrometer or nanometer scale. Study of the preparation and properties of various nanostructured materials has received extensive attention during the last two decades [1]. In this article, we report a novel method to synthesize ultrafine-layered lanthanon titanates ($K_2Ln_2Ti_3O_{10}$ Ln = La, Nd, Gd, Sm, Dy) and photocatalytic properties of this material.

$K_2Ln_2Ti_3O_{10}$ (Ln = La, Nd, Gd, Sm, Dy), a layered perovskite-type compound with a hydrated interlayer space, is one type of the most extensively studied photocatalytic material [2–9] because of its better photoreactivity comparing with TiO_2. As a catalyst, high dispersibility and large surface area are crucially important. However, the actual particle size of $K_2Ln_2Ti_3O_{10}$ was usually at least on the micrometer scale because they were usually prepared via a solid-state reaction (SSR) of K_2CO_3, Ln_2O_3 and TiO_2 at high temperature (1100–1300 °C) with long reaction time [2,4–9]. So the control of its preparation is always a key point for obtaining excellent photoactivities [10]. Because of the difficulty in preparing ultrafine-layered $K_2Ln_2Ti_3O_{10}$ by the conventional SSR, little attention has been paid to investigating the change of the structure and the properties of these compounds when the particle size of these compounds becomes smaller.

One of the typical strategies to synthesize nanoscale complex oxides is using precursor routes [1]. We previously reported a non-hydrolytic method, the so-called stearic acid method (SAM) to prepare various

*Corresponding author. Fax: +86 25 84315054.
E-mail address: zhanglily800@yahoo.com.cn (L. Zhang).

0022-4596/$ - see front matter © 2004 Elsevier Inc. All rights reserved.
doi:10.1016/j.jssc.2004.12.024

nanocrystalline complex oxides using stearic acid as reactant and dispersant [11–14]. It was found that various metallic ions could be dispersed at the molecular level in melted stearic acid via a liquid-state mixing process, and each component was uniformly mixed even in the resulting product after removing organic substances by combustion. This could remarkably reduce the SSR reaction temperature and the ultrafine complex oxides could be easily obtained. Herein, we developed this technique to fabricate ultrafine $K_2Ln_2Ti_3O_{10}$ (Ln = La, Nd, Gd, Sm, Dy) powders. Results showed that $K_2Ln_2Ti_3O_{10}$ was successfully synthesized at a relatively low temperature with shortened reaction time and the d(002) values of obtained products were different from each other when Ln changed. Compared with the product of traditional SSR, the particle size of $K_2Ln_2Ti_3O_{10}$ synthesized by SAM is smaller; BET surface area is higher (more than 16.97 m^2/g) and the photoreactivity is better. At the same time, the photodecomposition rate of methyl orange catalyzed by $K_2Ln_2Ti_3O_{10}$ is strongly dependent on lanthanide, increasing in the sequence of La < Sm < Nd < Gd < Dy. A possible reason has been put forward.

2. Experimental

2.1. Preparation and characterization of samples

The fabrication procedure of ultrafine $K_2Ln_2Ti_3O_{10}$ (Ln = La, Nd, Gd, Sm, Dy) is illustrated in the flowchart in Fig. 1. Tetrabutyl titanate ($Ti(OBu)_4$), KOH and $Ln(NO_3)_3$(Ln = La, Nd, Gd, Sm, Dy) obtained from Ln_2O_3 dissolved in HNO_3 were used as the precursors of Ti, K and Ln, respectively. Concerning the volatilization of potassium during calcinations, the molar rate of K/Ln/Ti is 3.6/2/3 (containing 80% excess amount of potassium). Firstly, two appropriate portions of stearic acid (ca. 30 g) were heated and melted. A given amount of KOH and $Ln(NO_3)_3$ were added into them and were named as Solution A and Solution B separately. These mixtures were thoroughly stirred by the magnetic mixer to eliminate the water. Then Solution A was dumped into Solution B. After 0.5 h, an appropriate amount of $Ti(OBu)_4$ was added with vigorous stirring. Two hours later, a homogeneous transparent solution was formed. The solution was ignited in air and the obtained powders were calcined at a series of increasing temperatures ranging from 400 to 900 °C for 2 h in air.

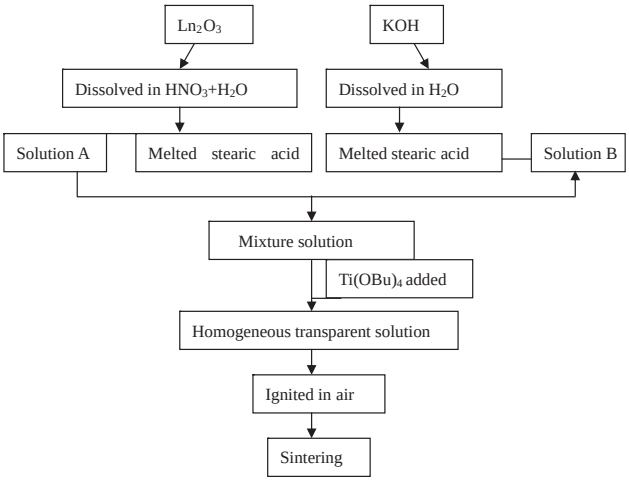

Fig. 1. Flowchart for chemical processing of $K_2Ln_2Ti_3O_{10}$ (Ln = La, Nd, Gd, Sm, Dy).

For comparison, $K_2Ln_2Ti_3O_{10}$ (Ln = La, Nd, Gd, Sm, Dy) was also synthesized by traditional SSR according to Ref. [2,6]. $K_2Ln_2Ti_3O_{10}$ was prepared from K_2CO_3, Ln_2O_3 and TiO_2 powders. These stoichiometric mixtures were first calcined at 900 °C for 5 h followed by grinding and calcination at 1100 °C for 11 h.

The preparative process was monitored by FT-IR spectroscopy with a Bruker Vector 22 spectrometer. The crystalline phase structure was determined by Bruker D8 Advance X-ray diffractometer (XRD) using Cu$K\alpha$ radiation. The BET surface area was evaluated by N_2 adsorption in a constant volume adsorption apparatus (Coulter SA 3100). The morphology was determined by scanning electron microscopy (SEM) and transmission electron microscopy (TEM) using LEO-1530VP SEM microscopy and H-800 TEM microscopy, respectively.

2.2. Photocatalytic activity measurement

The photoreactivities of the samples were evaluated by methyl orange decomposition under UV irradiation. A 300W high-pressure mercury lamp provided the irradiation with a wavelength centered at 365 nm. The initial concentration of methyl orange in a quartz reaction vessel was fixed at 20 mg/L with as-prepared catalysts loading of 1 g/L. The reaction cell (500 mL) was bubbled with air at a flow rate of 10 mL/min. The extent of methyl orange decomposition was determined by measuring the absorbance value at 465 nm using UV-1100 spectrometer.

3. Results and discussion

3.1. Characterization of the preparative process of SAM

In this work, $K_2Nd_2Ti_3O_{10}$ was taken as an example to describe the fabricating process prepared by SAM. Stearic acid is one widely used surfactant. Its carboxylic acid group and long-carbon chain endow it with strong ability to disperse various substances. In order to investigate the reaction and uniform distribution

mechanism of the reactant in the preparative process, FT-IR was utilized to monitor the structural changes of compounds during the preparative process. It was found that strong chemical interaction existed between metal precursors and stearic acid. After KOH was added into stearic acid, the characteristic absorption bands of –COOH (1702, 934.5 cm^{-1}) decreased while one band at 1560 cm^{-1} was observed, which is assigned to the stretching vibration of $–COO^-$ (see Fig. 2), indicating that potassium stearate was formed. After $Ti(OBu)_4$ was added to stearic acid, two new bands at 1590–1540 cm^{-1} appeared. The band at 1550–1590 cm^{-1} was attributed to the COO^- stretching vibration for bidenate Ti(IV)–carboxylic acid complex [11,12], indicating that strong coordination interaction between Ti(IV) and stearic acid existed. However, after $Nd(NO_3)_3$ was added into stearic acid, two characteristic absorption bands of NO_3^- (1545, 1304 cm^{-1}) were observed and no bands belonging to $–COO^-$ existed indicating that there was no reaction between Nd^{3+} and stearic acid; the stearic acid just acted as surfactant. Through the strong interaction and dispersion between metal elements and stearic acid, Ti(IV), K^+ and Nd^{3+} were uniformly dispersed in the stearic acid, attaining molecular-level distribution. The highly dispersed precursors may guarantee that the resulting $K_2Ln_2Ti_3O_{10}$ products are ultrafine.

Fig. 3 shows the DTA and TG curves of the precursor gel of $K_2Nd_2Ti_3O_{10}$. It can be seen that the DTA curve has five peaks: the first endothermic peak (60 °C) is associated with the melting of stearic acid, the second endothermic peak (249.68 °C) with relatively large weight loss (83%) is caused by the evaporation and burning of the organic substance, the third exothermic peak (349.04 °C) is attributed to the fabrication of intermediate state ($KNd_2Ti_3O_{9.5}$), the fourth small exothermic peak (425 °C) is relative to the crystal lattice energy released during the formation of perovskite-type structure and the largest endothermic peak with 3.49% weight loss is regarded as the volatilization of excess potassium, burning of remaining organic substance and the formation of $K_2Nd_2Ti_3O_{10}$ structure. The overall weight loss observed in Fig. 3 is 95.10%, which is quite consistent with the theoretical weight loss (94.88%), indicating the complete removal of all the stearic acids. No further peak or weight loss up to 800 °C was found, suggesting the $K_2Nd_2Ti_3O_{10}$ can be fabricated at about 700 °C. These results can be confirmed by the XRD patterns.

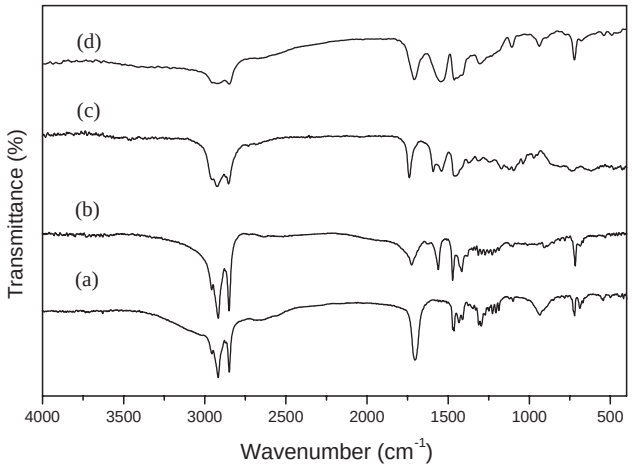

Fig. 2. FT-IR spectra of (a) stearic acid, (b) KOH + stearic acid, (c) $Ti(OBu)_4$ + stearic acid, and (d) $La(NO_3)_3$ + stearic acid.

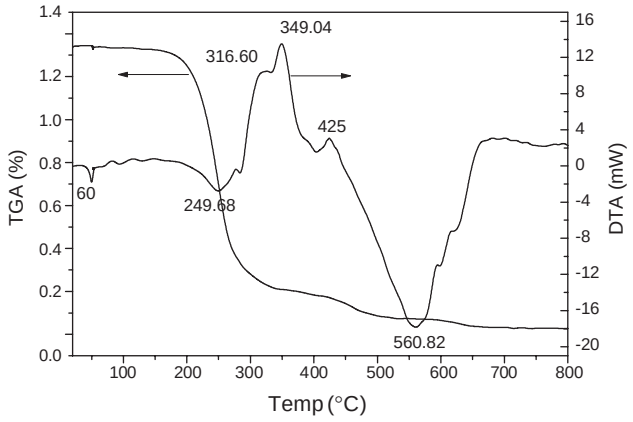

Fig. 3. DTA/TA curves of the precursor gel of $K_2Nd_2Ti_3O_{10}$.

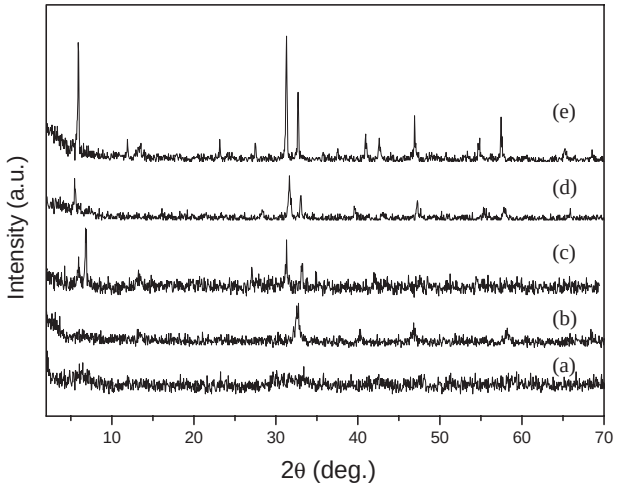

Fig. 4. XRD patterns of the (a) precursor powder ignited in air and the products calcined at a series of increasing temperatures of $K_2Nd_2Ti_3O_{10}$, (b) 500 °C, 2 h, (c) 700 °C, 2 h, (d) 800 °C, 2 h, and (e) 800 °C, 6 h.

A clear transition from amorphous state to crystalline state could be noticed in Fig. 4. The basic powder is amorphous but containing a small amount of $KNd_2Ti_3O_{9.5}$ (JCPDS 430595) as a mediate phase. When heated at 500 °C, the intermediate product of $KNd_2Ti_3O_{9.5}$ was very clear indicating the elevated

temperature was required to yield $K_2Nd_2Ti_3O_{10}$ powders. We detected the first appearance of perovskite-type structure when the sample was heated at 700 °C, but the crystallinity was quite low. As the temperature was raised to 800 °C and the calcination time was extended to 6 h, a single phase of $K_2Nd_2Ti_3O_{10}$ (JCPDS 870479) was completely formed. The fabrication process of other $K_2Ln_2Ti_3O_{10}$ (Ln = La, Gd, Sm, Dy) was very similar to this. The only difference was that $K_2Dy_2Ti_3O_{10}$ crystalline did not appear only when the precursor had been heated at 900 °C for 6 h. These results suggest that the $K_2Ln_2Ti_3O_{10}$ series, which usually forms at high temperatures in conventional method (~1100 °C) with a long reaction time, can be successfully synthesized at a relatively low temperature with shortened reaction time by using SAM.

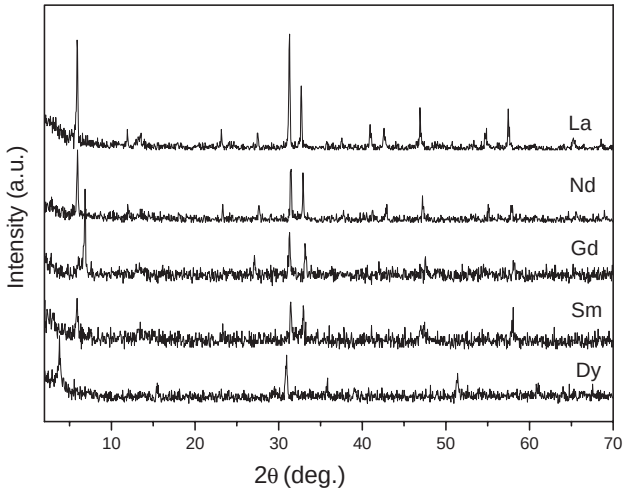

Fig. 5. XRD patterns of $K_2Ln_2Ti_3O_{10}$ (Ln = La, Nd, Sm,Gd, Dy).

Fig. 5 shows the XRD patterns of $K_2Ln_2Ti_3O_{10}$ prepared by SAM. The La compound consisted of a single phase of layered perovskite $K_2La_2Ti_3O_{10}$, the XRD pattern of which is indexed based on tetragonal lattice (I_4/mm, $a = 3.871$ Å, $c = 29.78$ Å) as reported previously [2,9]. This type of tetragonal-layered perovskite was also produced for Ln = Nd, Sm, Gd, Dy, being free from the starting materials or other impurities. But the crystallinities of $K_2Ln_2Ti_3O_{10}$ differ from each other when the Ln changes because of the different reactive characteristics of Ln and varied heating temperature (see Table 1). For Ln = La, it may be easy to achieve the reaction balance, but for Ln = Sm, it may be relatively hard to obtain the perovskite structure under the same condition.

3.2. Influence of preparation method on the microstructure of prepared $K_2Ln_2Ti_3O_{10}$ powders

Preparative methods have a great effect on the crystal structure of the obtained products. Table 1 summarizes the main parameters of obtained $K_2Ln_2Ti_3O_{10}$ crystalline prepared by SAM. First of all, it can be seen that the values of d(002) increase along with the atomic number from La to Dy, in spite of Ln = Gd (also can be seen in Fig. 5). It is difficult to understand this difference. To the best of our knowledge, one possible reason is that the Ln^{3+} $4f$ levels have great effect on the lattice structure. The d(002) value of $K_2Ln_2Ti_3O_{10}$ tends to increase with the enhancement of Ln^{3+} $4f$ electron numbers in spite of Gd^{3+} because its $4f^7$ is half-filled (see Table 2). The other reason is that the ionic radius of

Table 1
Main parameters of obtained $K_2Ln_2Ti_3O_{10}$ crystallite by SAM

Main parameters	La	Nd	Sm	Gd	Dy
d(002) (nm)	1.476	1.479	1.497	1.295	2.319
BET surface area (m^2/g)	11.83	16.97	12.35	13.04	10.59
Average size (nm × nm)	500 × 450	225 × 250	300 × 500	160 × 230	1400 × 1100
Reaction temperature (°C)	800	800	800	800	900
Calcination times (h)	3	6	8	8	6

Table 2
Ionic information, band gap and photoreactivity of $K_2Ln_2Ti_3O_{10}$

Ln^{3+}	d(002) (nm)	Ionic radius (Å)	Valence shell of Ln^{3+}	E_g (eV)	Photodegraded amounts of methyl orange by $K_2Ln_2Ti_3O_{10}$ in 2 h (%)
La	1.476	1.032	[Xe]	3.05	10.8
Nd	1.479	0.983	$4f^3$	3.25	17.9
Sm	1.497	0.985	$4f^5$	3.26	12.7
Gd	1.295	0.938	$4f^7$	3.30	20.4
Dy	2.319	0.912	$4f^9$	3.38	44.8

lanthanon affects the structure of $K_2Ln_2Ti_3O_{10}$. As can be seen in Table 2, the value of $d(002)$ increases along with the decreases of ionic radius from La^{3+}, Nd^{3+}, Sm^{3+} to Dy^{3+} (in spite of Gd). But in our experiment, we found that it was impossible to achieve the layered perovskite structure of $K_2Ln_2Ti_3O_{10}$ when using Er ($rEr^{3+} = 0.890$ Å) to replace Ln. This result suggests that the formation of layered perovskite in $K_2Ln_2Ti_3O_{10}$ system is dependent on the ionic radius of Ln^{3+} [16] there must exist a range of r_{Ln} to obtain this structure. Further work is under progress.

Preparative methods also influence the grain size and dispersibility of the obtained powders. Fig. 6 shows the TEM and selected area electron diffraction micrographs of the sample prepared by SAM. The product of $K_2La_2Ti_3O_{10}$ crystalline is quadrilateral and with good dispersibility, which is consistent with Ref. [7,8] and the electron diffraction of the freshly prepared $K_2La_2Ti_3O_{10}$ reveals that the sample is a single crystal body-centered tetragonal $K_2La_2Ti_3O_{10}$. The average size of $K_2La_2Ti_3O_{10}$ estimated from TEM is 500 nm × 450 nm. These results are confirmed by SEM images as well. From the picture of both Fig. 7 (a) and (b), we can clearly see the unique layered structure of $K_2La_2Ti_3O_{10}$ (see the arrow in Fig. 7) and both of them are square-like. But the average grain size of $K_2La_2Ti_3O_{10}$ obtained by SAM is about 500 nm × 450 nm, which is quite smaller than that of the solid-state method (ca. 1.5 μm × 1 μm).

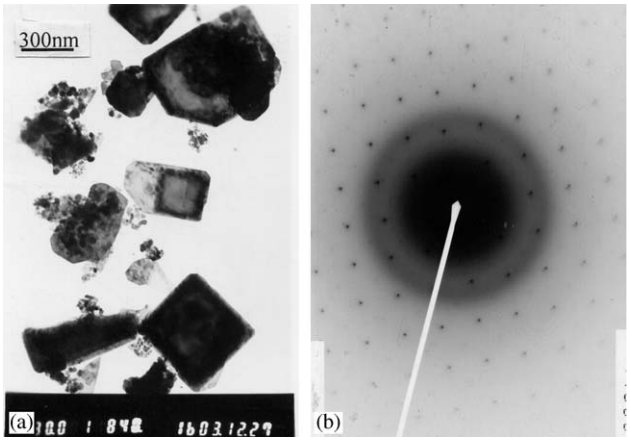

Fig. 6. (a) TEM micrograph, and (b) electron diffraction pattern of $K_2La_2Ti_3O_{10}$ prepared by SAM obtained at 800 °C.

Fig. 8 showed the SEM micrographs of other $K_2Ln_2Ti_3O_{10}$ (Ln = Nd, Sm, Gd, Dy) crystalline prepared by SAM. It is very clear that the products with high dispersibility are all square-like and have a unique layered structure (see the arrows in Fig. 8), which are in good consistency with Ln = La and Ref. [7,8], indicating that the crystallinity of the products is quite well. As can be seen, the average sizes of obtained products ranged from 300 to 1000 nm for Ln = Nd, Sm, Gd, Dy separately (see Table 1). And for Ln = Dy, it has the largest average size because it was fabricated at the highest temperature.

Meanwhile, the BET surface areas of $K_2Ln_2Ti_3O_{10}$ calculated from N_2 isotherms at −196 °C were in the range of 10–18 m^2/g (see Table 1), which are larger than those prepared by traditional SSR (~1 m^2/g) [3]. So these good physical properties of obtained samples by SAM, such as more regular morphology, higher dispersibility and larger BET surface area, etc. may result in better behavior in photocatalytic reaction.

3.3. Photocatalytic activity measurement

Photoactivity is one of the typical properties of $K_2Ln_2Ti_3O_{10}$ and the property was strongly dependent on the surface structure and the catalytic property of the material itself. As-prepared $K_2Ln_2Ti_3O_{10}$ series were used to photodecompose methyl orange without any further pretreatments. Fig. 9 shows that the photocatalytic reaction goes with irradiation time using $K_2Ln_2Ti_3O_{10}$ (Ln = Dy, Gd) as catalyst. Apparently, the plot is linear indicating that this photocatalytic reaction is a first-order reaction. The photoreactivity of other $K_2Ln_2Ti_3O_{10}$ is very similar to this, but the

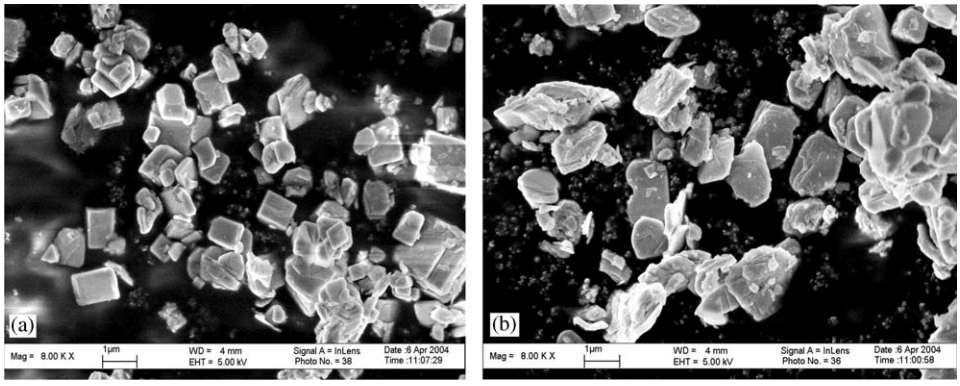

Fig. 7. SEM micrographs of $K_2La_2Ti_3O_{10}$ prepared by (a) SAM, and (b) SSR.

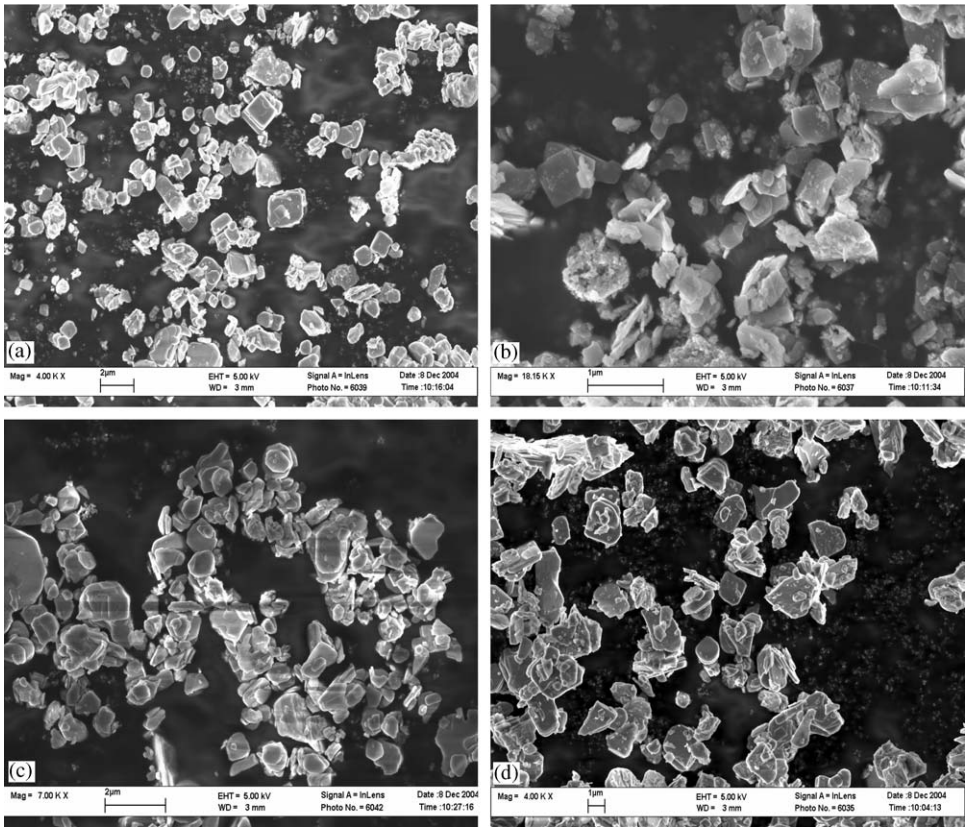

Fig. 8. SEM micrographs of products prepared by SAM (a) $K_2Nd_2Ti_3O_{10}$, (b) $K_2Sm_2Ti_3O_{10}$, (c) $K_2Gd_2Ti_3O_{10}$, and (d) $K_2DyTi_3O_{10}$.

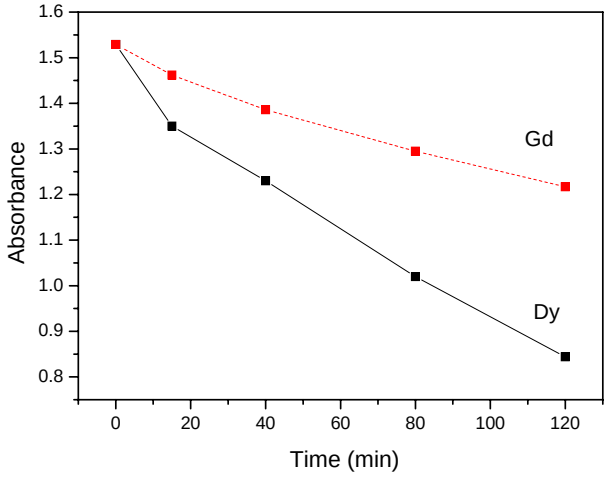

Fig. 9. Absorbance of methyl orange catalyzed by $K_2Ln_2Ti_3O_{10}$ with irradiation time.

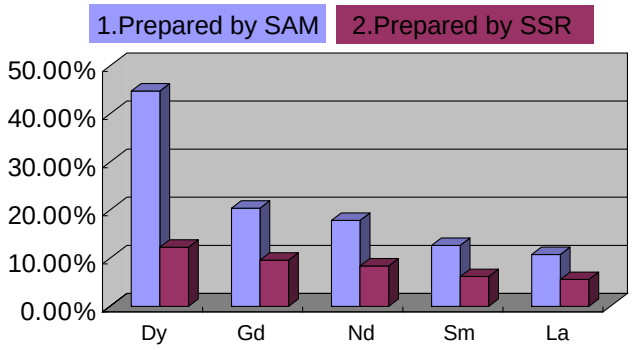

Fig. 10. Photodegraded amounts of methyl orange by $K_2Ln_2Ti_3O_{10}$ in 2 h.

decomposition rates are different from each other when *Ln* changes. Fig. 10 summarized the photodegraded amounts of methyl orange catalyzed by $K_2Ln_2Ti_3O_{10}$ in 2 h, which was fabricated by both SAM and SSR. It was found that the photoactivities of samples obtained by SAM are all better than those of SSR accordingly because of their better physical properties mentioned above (see Table 1). However, it is interesting to find that the photodegraded amount of methyl orange was strongly dependent on *Ln*, decreasing in the sequence of Dy > Gd > Nd > Sm > La by the same method. In the Dy case, the photodecomposition rate of methyl orange is 44.8%, whereas in the case of La the decomposition rate decreased to 10.8%.

This phenomenon was also found in other systems, such as $RbLnTa_2O_7$ [15,16]. It is difficult to rationalize the sequence of this system. Most important of all, this is considered [15,16] largely to be a consequence of the partly occupied *Ln4f* levels, which form narrow bands

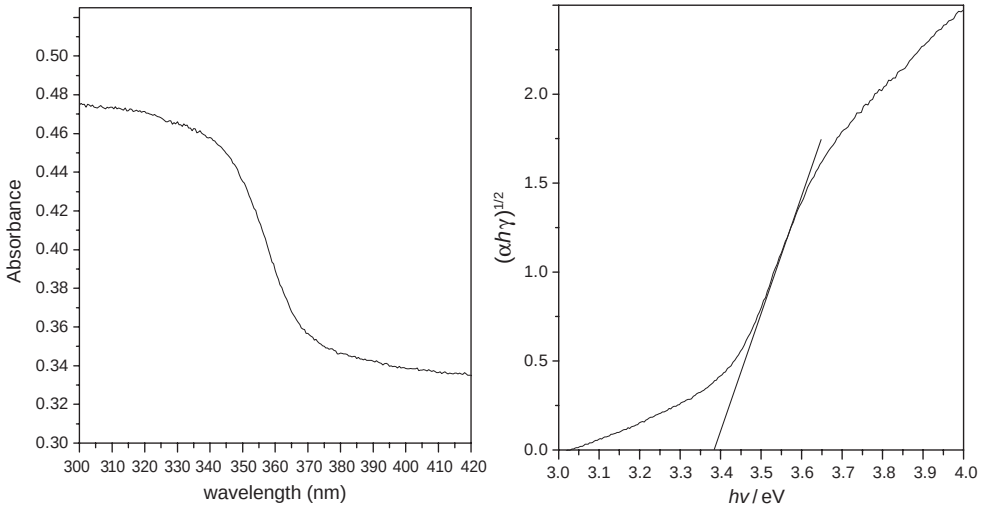

Fig. 11. (a) UV–visible absorption spectra of $K_2Dy_2Ti_3O_{10}$ prepared by SAM, and (b) $(\alpha h\gamma)^2$ versus $h\nu$ and showing the fit to linear portion corresponding to the direct band gap transition.

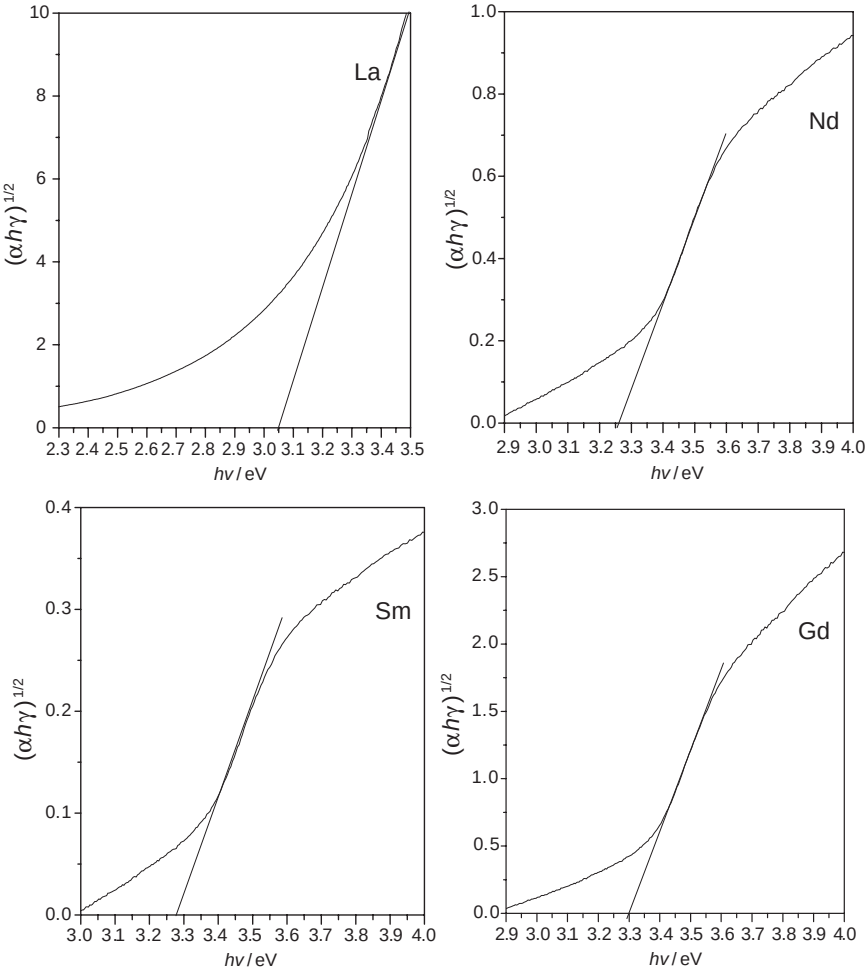

Fig. 12. $(\alpha h\gamma)^{1/2}$ versus $h\nu$ and showing the fit to linear portion corresponding to the direct band gap transition of $K_2Ln_2Ti_3O_{10}$(Ln = La, Nd, Sm, Gd) prepared by SAM.

within the band gap of the Ti–O sublattices. This may imply that photoexcited *Ln4f* electrons play a key role in the photocatalysis of the present layered pervoskite lanthanon titanates [16,17] and it is materialized in the form of the band gap.

Fig. 11a shows the representative UV–vis absorbance spectra of $K_2Dy_2Ti_3O_{10}$ crystalline in 50%(v/v) glycol/water suspension prepared using 20 W/cm^2 sonic intensity. The optical data were analyzed at the near-absorption edge using the equation

$$a = K(hv - E_g)^{n/2}/hv,$$

where K and n are constants and E_g is the band gap of the semiconductors [17]. The value of n is equal to 1 for a direct band gap material, whereas $n = 4$ for an indirect transition material. In $K_2Ln_2Ti_3O_{10}$, there are two possibilities of charge transfer transition involving *4f* levels, i.e., from the highest filled (valance) band mainly composed of O*2p* to the *Ln4f* levels, or from the *Ln4f* levels to the conduction band. In such cases, the resultant photoexcited electrons or holes may take part in the catalytic reaction on the surface. Actually, however, the direct electron transfers from *Ln4f* to the conduction band would be impossible due to a large inteatomic distance (*Ln*–Ti) [9]. In contrast, *Ln4f* may interact with the O*2p* (*Ln*–O) that participates in deriving the conduction band through Ti–O–Ti interactions [16]. In this regard, n should be fixed at 4. Apparently, the plot of $(\alpha hv)^{1/2}$ versus hv (Fig. 11b) gives E_g for an indirect allowed transition when the linear region is extrapolated to zero ordinate. So the estimated E_g of $K_2Dy_2Ti_3O_{10}$ was about 3.38 eV. The band gap of other lanthanides tested by the same method was shown in Fig. 12 and summarized in Table 2. It was found that the photoactivity sequence of $K_2Ln_2Ti_3O_{10}$ was well reflected by the band gap energy as shown in Table 2. The higher band gap is, the better the photoreactivity will be. And $Ln = Dy$ ($E_g = 3.38$ eV) has the maximum photoreactivity which is in accordance with the irradiation of 365 nm (about 3.4 eV).

On the other hand, the photocatalytic activity is dependent on the crystallinity of the catalyst. Thus, the low activity for $Ln = Sm$ might be due to its poor crystallinity when compared with $Ln = Nd$, Gd. But on considering that the crystallinity of $Ln = La$ is the highest but its photoactivity is the poorest, we think that the photocatalytic activity of $K_2Ln_2Ti_3O_{10}$ was strongly dependent on *Ln* and the crystallinity was the second place effect. Clearly, however, further detailed study and more electronic informations are necessary to understand this photocatalytic sequence.

Acknowledgments

The authors thank the Doctoral and Postdoctoral Science Foundations of the Department of Education of China and the Doctoral Creative Project of Jiangsu Province for financial support.

References

[1] H.S. Nalwa (Ed.), Handbook of Nanostructured Materials and Nanotechnology, Academic Press, San Diego, 1999.
[2] J. Gopalakrishnan, B. Vasodeva, Inorg. Chem. 26 (1987) 4299.
[3] D. Kazunari, N.K. Junko, A. Michikazu, T Tsuyoshi, Bull. Chem. Soc. Japan 73 (2000) 1307.
[4] W.H. Dong, G.K. Hyun, J. Catal. 193 (2000) 40.
[5] Wenfeng Shangguan, Akira Yoshida, Int. J. Hydrogen Energy 24 (1999) 425.
[6] T. Takata, K. Shinohara, A. Tanaka, et al., J. Photochem. Photobiol. A: Chem. 106 (1997) 45.
[7] R.E. Schaak, T.E. Mallouk, Chem. Mater. 12 (2000) 3427.
[8] R.E. Schaak, T.E. Mallouk, Chem. Mater. 12 (2000) 2513.
[9] S.H. Byeon, H.J. Nam, Chem. Mater. 12 (2000) 1771.
[10] C. Legros, C. Haut, L. Ponsonnet-Mora, J. Ayache, J. Eur. Ceram. Soc. 19 (1999) 165.
[11] G. Xiong, Z.L. Zhi, X.J. Yang, et al., J. Mater. Sci. Lett. 16 (1997) 1064.
[12] J. Yang, D. Li, X. Wang, et al., J. Solid State Chem. 165 (2002) 193.
[13] J. Yang, D. Li, X. Wang, et al, Mater. Sci. Eng. A 328 (2002) 108.
[14] L.L. Zhang, J. Yang, W.G. Zhang, et al., Chin. J. Inorg. Chem. 19 (2003) 1217.
[15] M. Machida, J. Yabunaka, T. Kijima, et al., Int. J. Inorg. Mater. 3 (2001) 545.
[16] M. Machida, J. Yabunaka, T. Kijima, Chem. Mater. 12 (2000) 812.
[17] J.J. Zhu, H. Wang, S. Xu, et al., Langmuir 18 (2002) 3306.